A photo-SAR study of photoswitchable azobenzene tubulin-inhibiting antimitotics identifying a general method for near-quantitative photocontrol

Martin Reynders[1], Małgorzata Garścia[1], Adrian Müller-Deku[1], Maximilian Wranik[3], Kristina Krauskopf[1], Luis de la Osa de la Rosa[1], Konstantin Schaffer[2,4], Anna Jötten[2,4], Alexander Rode[1], Valentin Stierle[2], Yvonne Kraus[1], Benedikt Baumgartner[1], Ahmed Ali[1], Andrei Bubeneck[1], Trina Seal[1], Michel O. Steinmetz[3,5], Philipp Paulitschke[2,4], Oliver Thorn-Seshold[1,*]

[1] Faculty of Chemistry and Pharmacy, Ludwig-Maximilians-University Munich, Munich 81377, Germany
[2] Faculty of Physics and Center for NanoScience (CeNS), Ludwig-Maximilians-University Munich, Munich 80539, Germany
[3] Laboratory of Biomolecular Research, Division of Biology and Chemistry, Paul Scherrer Institut, Villigen 5232, Switzerland
[4] PHIO scientific GmbH, Munich 81371, Germany
[5] Biozentrum, University of Basel, Basel 4056, Switzerland
* Correspondence and requests for materials: oliver.thorn-seshold@cup.lmu.de
Keywords*: tubulin inhibitors, microtubule dynamics, antimitotics, photopharmacology, photoswitches, sensitisation, azobenzenes*

Abstract

Azobenzene analogues of the tubulin polymerisation inhibitor combretastatin A4 (**PSTs**) were previously developed to optically control microtubule dynamics in living systems, with subsecond response time and single-cell spatial precision, by reversible *in situ* photoswitching of their bioactivity with near-UV/visible light. First-generation **PSTs** were sufficiently potent and photoswitchable for use in live cells and embryos. However, the link between their seconds-scale and hours-scale bioactivity remained untested. Furthermore, the scope for modifications to tune their photo-structure-activity-relationship or expand their function was unknown. Here, we used large-field-of-view, long-term tandem photoswitching/microscopy to reveal the timing of onset bulk cytostatic effects. We then synthesised a panel of novel PSTs exploring structural variations that tune photoresponse wavelengths and lipophilicity, identifying promising blue-shifted analogues that are better-compatible with GFP/YFP imaging. Taken together, these results can guide new design and applications for photoswitchable microtubule inhibitors. We also identified tolerated sites for linkers to attach functional cargos, and tested them with fluorescent "antennas" as reporters. Serendipitously, we found that antennas can greatly enhance long-wavelength single-photon photoisomerisation, by a hitherto unexplored mechanism. This final result will drive progress towards near-quantitative long-wavelength photoswitching of photopharmaceuticals in living systems, with minimal molecular redesign and general application scope.

Introduction

Microtubules (MTs) are major cytoskeletal components whose structure and dynamic remodelling are vital for diverse processes, from intracellular transport and cellular motility to the form and function of the mitotic spindle during proliferation.[1] The protein tubulin, which forms MTs, is highly conserved across all eukaryotes, and attempts to genetically modify the tubulin protein for direct stimulus-responsive control over its function have not been successful. Although genetic tools are recently being developed,[2–4] small molecule inhibitors that interfere with MT structure and dynamics remain indispensable as research tools for manipulating cytoskeleton biology.[5] In medicine too, MT inhibitors are successful antimitotic chemotherapeutics, particularly the taxane and vinca site binders;[6,7] while inhibitors binding at the colchicine site, including colchicine, combretastatin A-4 (**CA4**, **Fig 1a**), and their closely isosteric analogues, have also entered late-stage clinical trials.[8]

However, it is challenging or impossible to use these small molecule drugs study particular roles of MTs – e.g., in specific cell regions, cell populations or tissues, and at precisely defined times – since they cannot be either spatially or temporally directed.[9] Indeed, many important aspects of cytoskeleton biology remain poorly understood. Developing spatiotemporally-targetable small molecule MT inhibitors has thus been an important goal, and optical control strategies have been prioritised since light can be applied with high spatiotemporal precision even *in vivo*.[10,11] Irreversibly photo-triggered strategies were initially developed, including photobleachable and photouncageable inhibitors, or using practically irreversible C=C double bond photoisomerisation.[12–17] However, irreversibly triggered approaches cannot overcome the diffusion of the active drug over time, so they suffer conceptually from limited spatiotemporal resolution.

Spatially and temporally patterning bioactivity instead demands switching *in situ* in live cells, over many off↔on cycles. Azobenzene-based "**PSTs**" that are structural analogues of combretastatin A-4 are the best-developed platform for reversibly switchable tubulin polymerisation inhibitors. **PSTs** can be reversibly

photoswitched between their bioinactive *trans* and their up to >100-fold more potent *cis* isomers,[18] with excellent photostability, by low intensity near-UV and visible light: a combination of features that out-performs almost[19] all other photoresponsive MT inhibitors[20]. In biology, **PSTs** can photocontrol MT architecture, dynamics, and many MT-dependent processes in living cells with excellent spatiotemporal precision.[21,22] Streu,[23] Hartman,[24] Rastogi and Brittain[25] reported complementary aspects of **PST** biochemistry; and we have applied soluble and *in vivo*-compatible prodrugs **PST-1P** and **PST-2S** (**Fig 2a**) to study complex phenomena in cultured cells[26,27] and in developing embryos.[28,29]

Despite these applications,[21] there is much room to improve the utility of **PSTs** as tool compounds. For this, the chemical space for **PSTs** must first be characterised and understood. Though structure-activity-relationships (SAR) for combretastatin-like stilbenes are well known,[30] *cis*-**PST** potency is affected by unique factors that do not apply to the isosteric stilbenes (e.g., **PSTs** have >20-fold lower potency than expected, for reasons that are still unclear), and **PST** *cis*⇄*trans* switching adds new dimensions of structure-property relationships that must be balanced for performance. Therefore, we aimed to explore SAR and photophysical tuning of bioactive **PST** derivatives in a "photo-SAR" or PSAR study, in three areas: (i) classical SAR, to find the restraints on *cis*-**PST** structure needed to keep their potency useful within their solubility range; (ii) chemical biology, to find what modifications for developing multi-functional tool compounds are tolerated; (iii) photochemistry, to modify their practical performance (e.g., incremental absorption band shifting through substitutions, or larger modifications that test the limits of what photostationary states can be accessed in bioactive derivatives). Rastogi and Brittain[25] have made the only other systematic study of **PST** derivatives, though mostly this was limited to varying *meta*-substituents on the B ring, which is a separate scope of structural explorations that complements the PSAR developed here.

Finally, even the link between rapid-onset MT-inhibiting effects seen in live cell imaging assays (< seconds), and the long-term antimitotic effects that are the only cellular readout assessed in most photopharmacology studies (since easily and cheaply done in parallel throughput), has not been convincingly explored for this compound class (or indeed for most other photopharmaceuticals). However, it is necessary to confirm that the transition from short-term to long-term effects is indeed mechanistically linked, before one can be confident that cheap long-term assays can guide reagent development for the painstaking short-term imaging and photocontrol studies where reagents are ultimately supposed to perform. We therefore resolved to begin by monitoring this transitional link in time.

Results and Discussion

Time-dependency of photopharmaceutical effects

Like many photopharmaceuticals, **PSTs** undergo *Z*→*E* relaxation over time. In short-term assays where MT dynamics are monitored *directly*, this is usually irrelevant since high-intensity bidirectional isomerisations are used to jump between photostationary states (PSSs). However, in long-term assays (>24 hours) where *indirect, downstream* effects such as cell death are monitored, illuminations are often applied by low intensity light pulses every 1-5 minutes, aiming to build up and maintain a PSS throughout the experiment. As far as we know, no studies have explored the time-dependency of these readouts, so we were motivated to find out (1) how much *E*→*Z* illumination time is needed for cellular responses to be detectable via the usual long-term readouts (combines progressive *E*→*Z* isomerisation with cell inhibition); and (2) how much time is needed during dark phases for cells to resume normal behaviour (combines *Z*→*E* relaxation with biological recovery).

Such experiments would be highly time-consuming in endpoint assays (needs a great many endpoints to trace evolution over time), or in typical microscopy (small fields of view mean only few cells can be tracked in parallel). However, reconstruction-free lensless microscopy (RFLM) is ideally suited to track large numbers of cells non-invasively in parallel in such longitudinal assays. RFLM setups can be very compact (10×10×15 cm) and can simply be placed in an ordinary cell culture incubator to image and track thousands of cells per condition[31], over many conditions in parallel (here, eight). We modified an RFLM setup to co-apply 380 nm light at typical long-term low-intensity settings, during defined phases, for *in situ E*→*Z* photoswitching.

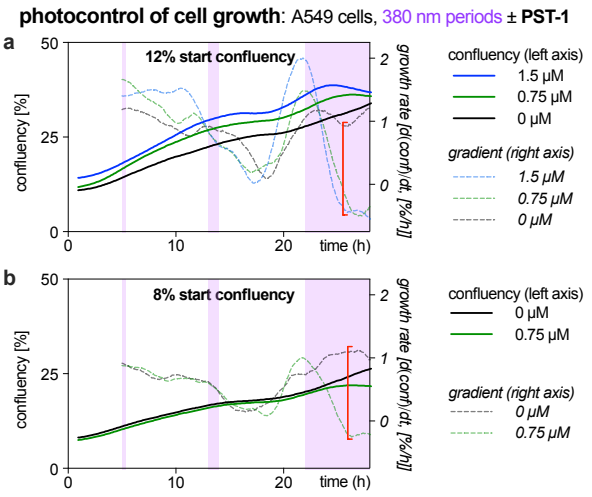

Figure 1. Exposure time-dependent onset of antimitotic effects with *Z*-**PST-1**. A549 lung cancer cells seeded at **(a)** 12% or **(b)** 8% confluency were treated with **PST-1**, and pulsed irradiations at 380 nm were applied during the purple-boxed timespans (durations 20 min, 1 h, or >6 h respectively; monitoring by RFLM).

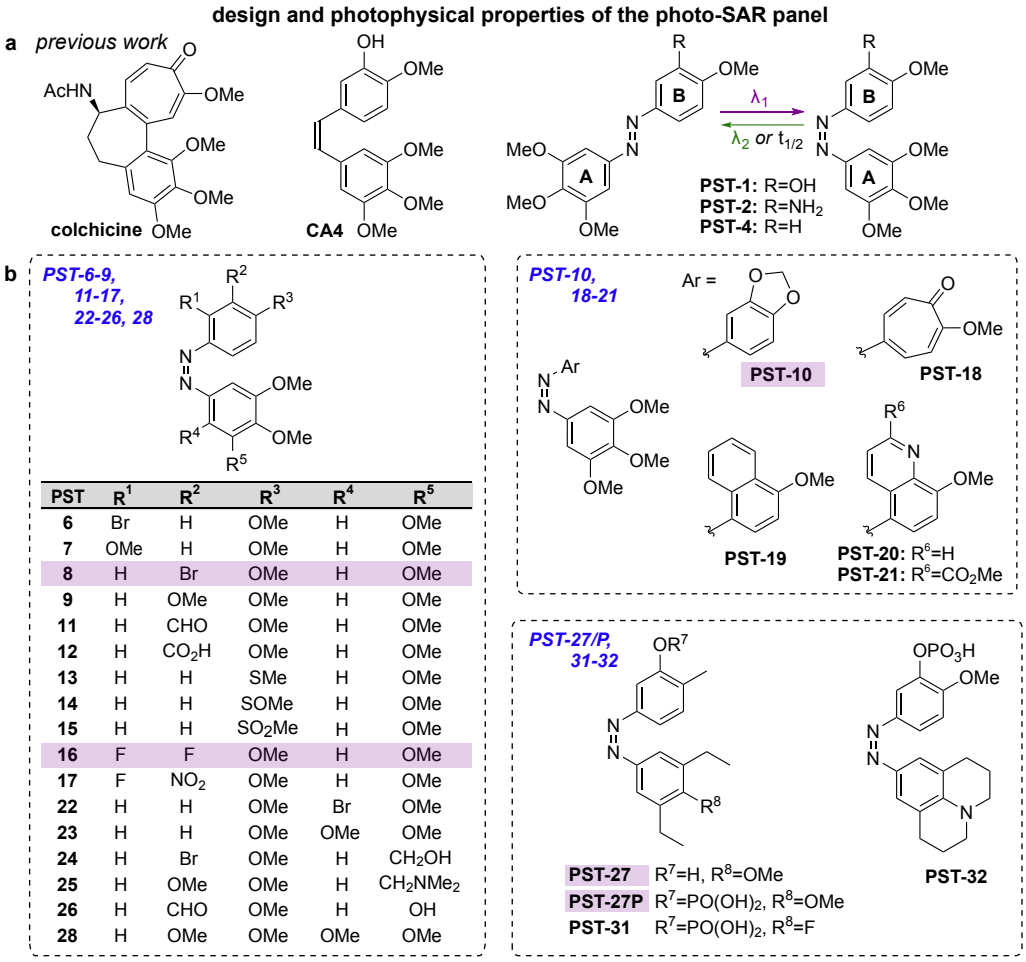

PST	R^1	R^2	R^3	R^4	R^5
6	Br	H	OMe	H	OMe
7	OMe	H	OMe	H	OMe
8	H	Br	OMe	H	OMe
9	H	OMe	OMe	H	OMe
11	H	CHO	OMe	H	OMe
12	H	CO_2H	OMe	H	OMe
13	H	H	SMe	H	OMe
14	H	H	SOMe	H	OMe
15	H	H	SO_2Me	H	OMe
16	F	F	OMe	H	OMe
17	F	NO_2	OMe	H	OMe
22	H	H	OMe	Br	OMe
23	H	H	OMe	OMe	OMe
24	H	Br	OMe	H	CH_2OH
25	H	OMe	OMe	H	CH_2NMe_2
26	H	CHO	OMe	H	OH
28	H	OMe	OMe	OMe	OMe

c

photophys.	PST-1	PST-8	PST-9	PST-16	PST-18*	PST-19	PST-20	PST-23	PST-27
$\lambda_{max,\,E}$ [nm]	375	366	374	366	405	400	392	366	344
$\lambda_{isosbest}$ [nm]	455	442	457	455	482	506	487	468	427
$\lambda_{strong,\,E\rightarrow Z}$ [nm]	378	380	388	380	n.d.	400	398	378	372
$t_{1/2}$ [min]	6.2	26	36	280	1.2	4.8	3.2	180	100

Figure 2. Design, synthesis and photoswitching. **(a)** Parent structures: colchicine, **CA4**, and prior **PST-1/2/4**. **(b)** Initial PSAR panel. **(c)** Photoswitching of key compounds: peak *E*-absorbance wavelength $\lambda_{max,E}$; isosbestic point λ_{iso}; wavelength with max PSS %Z $\lambda_{strong,E\rightarrow Z}$; thermal relaxation half-life $t_{1/2}$. **PSTs** are drawn as *Z*-isomers for easier comparison to **CA4**. See also **Fig S1-S2** and **Table S1**.

With short photoactivation periods (20 min, 1 h) no effects on proliferation were detected. However, from ca. 3 h of photoactivation, antimitotic effects were notable, since growth rates (rate of change of confluency over time) became strongly dependent on presence or absence of **PST** (**Fig 1**, red brackets). This reassured us that the PSAR of PSTs would be reliably assessed in typical long-term assays (24-48 h), even though we expected them to have differences in their efficiencies of bulk photoisomerisation and rates of *Z*→*E* relaxation.

Design and Synthesis of a Photo-SAR Panel

The SAR of stilbene-type combretastatin analogues, and the X-ray structure of the combretastatin-tubulin complex, suggest that one A-ring *ortho* position, and a neighbouring *ortho* and *meta* position on the B-ring, should be the most tolerant of substitutions:[30,32] but this PSAR has not been tested for azobenzene analogues. We synthesised a panel of 29 novel azobenzenes and azoheteroarenes (**PST-6**–**32**, **Fig 2**) to test these structural variations, primarily by diazonium couplings (see **Supporting Information**). Their photophysical properties, including *E* and *Z* isomer absorption spectra, PSS compositions, wavelengths giving the highest proportion of *Z* isomer, reversibility of photoswitching, and *Z*→*E* relaxation half-lives $t_{1/2}$ in aqueous media, were determined *in vitro*[21,33] (key compounds in **Fig 2c**, others in **Table S1** and **Fig S1-S3**).

The compounds were screened for cytotoxicity in the HeLa cervical cancer cell line under both dark and 390 nm-illuminated conditions (**Fig 3, Fig S9**)[21]. Our priority was not to maximise *Z*-isomer potency but rather to identify the structural tolerance for *photoswitchably* bioactive **PSTs**, that are potent as the *Z* isomer (illuminated) yet have low toxicity as the *E* isomer (dark): which is needed for photoswitchable-tool compounds.

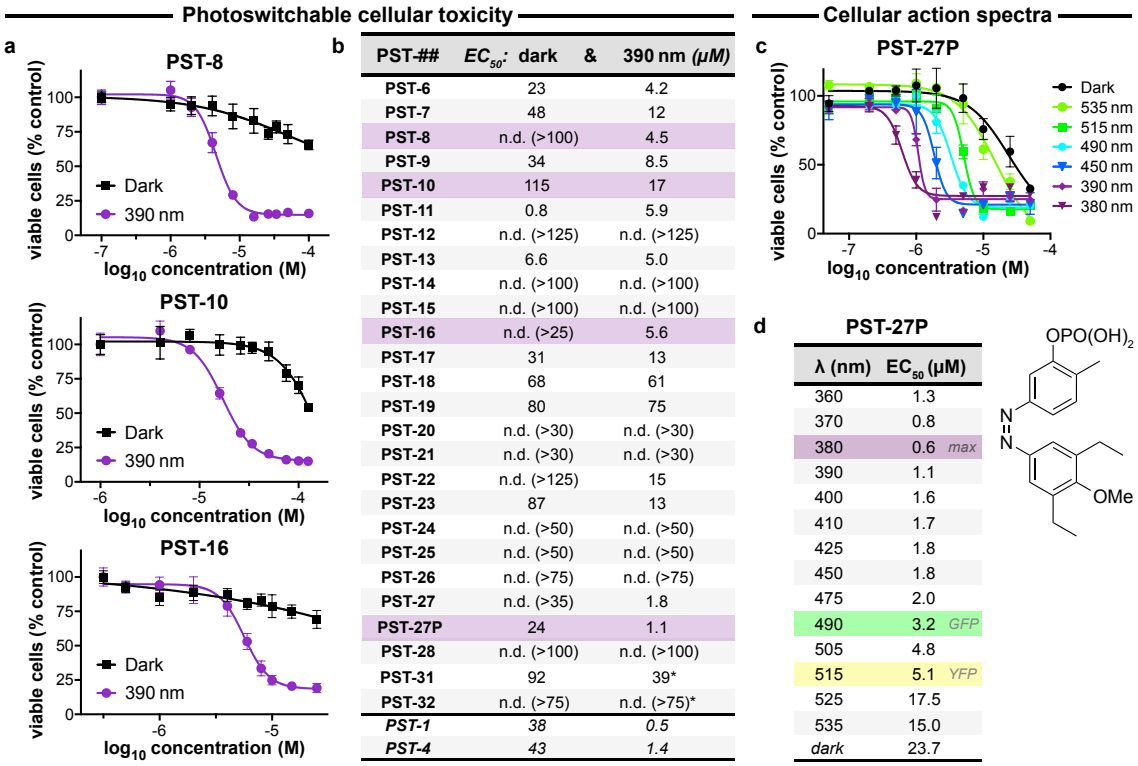

PST-##	EC_{50}: dark	& 390 nm (μM)
PST-6	23	4.2
PST-7	48	12
PST-8	n.d. (>100)	4.5
PST-9	34	8.5
PST-10	115	17
PST-11	0.8	5.9
PST-12	n.d. (>125)	n.d. (>125)
PST-13	6.6	5.0
PST-14	n.d. (>100)	n.d. (>100)
PST-15	n.d. (>100)	n.d. (>100)
PST-16	n.d. (>25)	5.6
PST-17	31	13
PST-18	68	61
PST-19	80	75
PST-20	n.d. (>30)	n.d. (>30)
PST-21	n.d. (>30)	n.d. (>30)
PST-22	n.d. (>125)	15
PST-23	87	13
PST-24	n.d. (>50)	n.d. (>50)
PST-25	n.d. (>50)	n.d. (>50)
PST-26	n.d. (>75)	n.d. (>75)
PST-27	n.d. (>35)	1.8
PST-27P	24	1.1
PST-28	n.d. (>100)	n.d. (>100)
PST-31	92	39*
PST-32	n.d. (>75)	n.d. (>75)*
PST-1	*38*	*0.5*
PST-4	*43*	*1.4*

PST-27P λ (nm)	EC_{50} (μM)	
360	1.3	
370	0.8	
380	0.6	*max*
390	1.1	
400	1.6	
410	1.7	
425	1.8	
450	1.8	
475	2.0	
490	3.2	*GFP*
505	4.8	
515	5.1	*YFP*
525	17.5	
535	15.0	
dark	23.7	

Figure 3. **PST** cytotoxicity can be optically controlled, with up to 20-fold enhancement from dark to lit conditions (MTT viability assay; HeLa cervical cancer cells; 46 h incubation). **(a)** Cell viability for selected **PSTs**. Data as mean ±SD. **(b)** EC_{50} values for all compounds (full data in **Fig S9**; *__PST-31__ irradiated at 370 nm and **PST-32** at 425 nm). **(c,d)** Wavelength-dependent cell viability with **PST-27P**.

Supporting Note 1 gives a full PSAR discussion. In brief however, for photoswitchability of bioactivity, the B ring tolerates small low-polarity groups at the *meta*-position (active bromo **8** but lower-potency alkoxy **9/10**, inactive carboxylate **12**); *ortho*-substituents are disfavoured although still have activity (**6** vs **7**); and if small, double substitution is allowed (difluoro **16**). Matching this, larger rings replacing the phenyl system that were reported for stilbenes[34–37] were not tolerated in the azobenzenes (**19-21**); so their alluring red-shifted photoresponse (**Fig 2c**) could not be harnessed. The A ring also tolerates small low-polarity *ortho*-substituents (**22**, **23**); but neither isosteric nor smaller *meta* groups are tolerated if they are polar (**24-26**).

Within this SAR range, multiple tolerated modifications can be made simultaneously. For example, **PST-27** was designed for blue-shifted photoresponse (less electron-rich), by replacing three methoxy groups with methyl/ethyls; this extra hydrophobicity required a B ring *meta* hydroxyl for solubility but became our most potently photoswitchably bioactive compound. This led us to prepare its highly water-soluble phosphate ester prodrug **PST-27P** for more reliable use in biology. We confirmed its strong wavelength-dependency of cytotoxicity over the entire range 360-535 nm (**Fig 3c-d**), supporting our premise that **PST** analogues' toxicities are determined by their *in situ* photoconversion to the bioactive *cis* isomer at PSS under the wavelength applied. Being blue-shifted, **PST-27P** had twice as good orthogonality to GFP/YFP excitation wavelengths (6-to-8 fold lower activity than max, **Fig 3d**) as compared to known **PST-1** (3-to-4 fold), which may make it more useful in many practical settings.[21] Unfortunately, the even more blue-shifted **PST-31** lost too much potency to be a useful tool compound; but we expect that strategies for further blue-shifting could be successful (e.g. a 3,4,5-triethyl A ring) in future work.

We next tested if the new **PSTs'** *cis* isomers retain tubulin inhibition as their primary mechanism of action (as for *Z*-**PST-1-5**[21]). Indeed, **PST-27P** gave light-specific disruption of MT network organisation at its cell viability EC_{50}, and gross MT depolymerisation above it (confocal imaging, **Fig 4a**), as did other well-performing compounds (**PST-8** and **PST-16**, **Fig 4b**). **PST-27** was progressed to further mechanistic tests, where it strongly inhibited microtubule assembly *in vitro* under 390 nm illumination, almost without perturbing polymerisation in the dark (**Fig 4c**). Cellular readouts downstream from MT inhibition were consistent with this mechanism of action: **PST-27P** gave light-specific accumulation of a sub-G_1 (dying) population (**Fig 4d**) consistent with the viability assay, accompanying a distinctive light-specific G_2/M phase arrest expected for cellular inhibition of tubulin dynamics (**Fig 4e-f**). Finally, we obtained an X-ray crystal structure of the metastable ***Z*-PST-27** bound to tubulin, confirming the same binding site and pose as the reference stilbene **CA4** (**Fig 4g**).

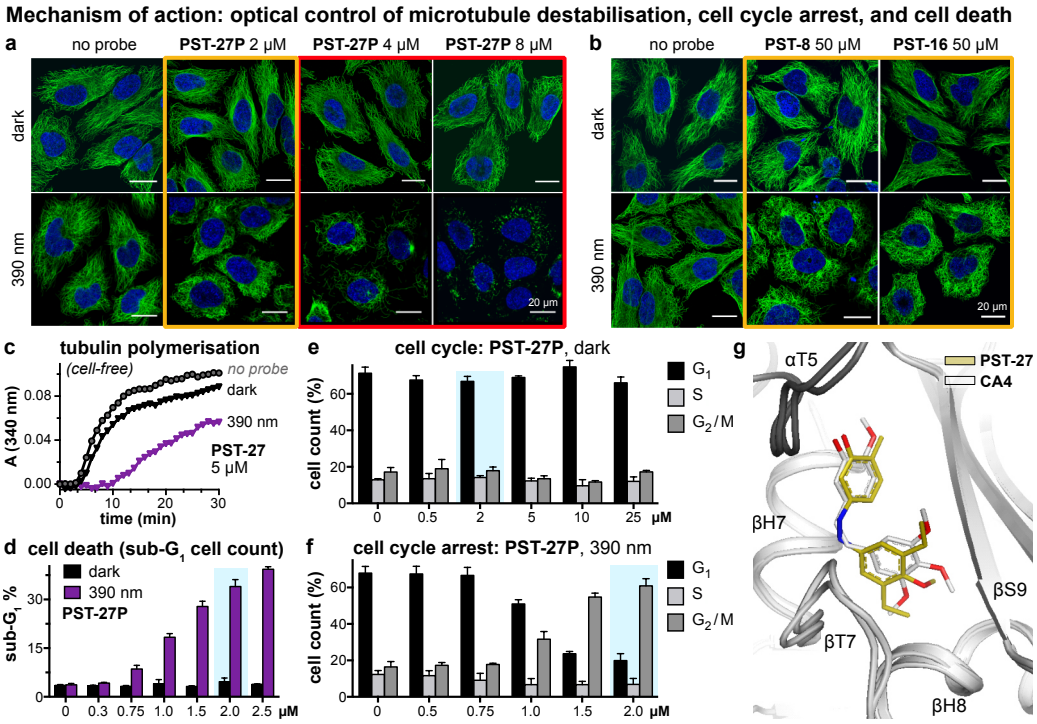

Figure 4. Mechanism of action assays show that *Z*-**PSTs**, but not *E*-**PSTs**, (**a**,**b**) induce microtubule network disorganisation [yellow frames] and depolymerisation [red frames], (**c**) inhibit polymerisation of purified tubulin protein, and (**d-f**) cause G_2/M phase cell cycle arrest and cell death [sub-G_1]. (**g**) X-ray crystal structure of αβ-tubulin:DARPin D1[38]:*Z*-**PST27** (olive carbons; PDB XXXX) superimposed on the tubulin:**CA4** complex structure (white carbons; PDB 5LYJ; rmsd = 0.584 Å). (**a**,**b**,**d-f**: in HeLa cells. **a**,**b**: 20 h treatment, α-tubulin immunostained with Alexa488 (green), DNA stained with DAPI (blue), scale bars 20 µm. **d-f**: data as mean ± SD).

Thus, we concluded that the *Z*-**PST** SAR and mechanism of action match those of known colchicine-site inhibitors.[30] We also saw that larger groups would be best tolerated in *ortho* at the A or B rings, and we aimed to exploit this for photoswitchably tubulin-binding **PST** conjugates with functional cargos. Here, we tested fluorophore-bearing conjugates, as model cargos that could also serve as light-dependent MT imaging agents (hope: *E:* distributed, *Z:* MT-bound). In brief, we attached fluorophores via linkers tethered to low steric demand ether and anilide groups at the *ortho* position of the A ring. We aimed for fluorophores with minimal absorption at 390 nm (**Fig S5a**), so that the conjugates might reach similarly *Z*-rich PSSs under UV illumination as the parent azobenzenes (later confirmed: **Fig 5b**) and so might be bioactive. For conjugate **MR110** we chose nitrobenzoxadiazole (NBD, ca. 450/550 nm ex/em); and for **MR69**[18] we chose an environment-independent rhodamine (RhB, ca. 530/560 nm ex/em, as a secondary amide that cannot form a nonfluorescent spirocycle) (**Fig 5a**). As the <500 nm tail of the NBD emission band overlaps with the absorption of *E*&*Z*-**PSTs** (**Fig S1-2**), we expected NBD excitation in **MR110** might drive **PST** isomerisation by resonant energy transfer (RET). However, for RhB excitation at e.g. 550 nm, the overlap with *E* and *Z* azobenzene isomers' absorption (<540 nm) should be near-zero, so we expected essentially no RET-based isomerisation for **MR69** (**Fig S5b**).

This expectation was dramatically overturned. **MR69** in particular was rapidly isomerised to high-*E*-content PSSs when the RhB fluorophore was excited (540-580 nm; **Fig S4**), i.e., with light to which the azobenzene does not respond (cf. **Fig 5d**: **PST-30** with 560 nm light).

In brief, key features of the conjugates include: **(1)** they have fast, efficient, *E*→*Z* photoswitching under UV light, as usual for azobenzenes (385 nm; **Fig 5b-d**). **(2)** Exciting the fluorophore motif gives exceptionally efficient switching (**Fig 5c**). **MR69** *Z*→*E* photoswitching above 550 nm approaches PSS with similar photon efficiency as its parent azobenzene does under UV light (effective switching half-lives in **Fig 5d**; ca. 0.5 min for >550 nm switching **MR69**, ca. 0.5 min for 400 nm switching **PST-30**). **(3)** Conjugate switching by exciting the fluorophore can be exceptionally complete: **MR69** reaches 94±3%*E* isomer at PSS 554 nm (compare typical azobenzenes that reach ca. 80%*E*). These are exciting results. Conjugate switching at long wavelengths can be orders of magnitude more photon-efficient (as well as more complete) than direct *Z*→*E* photoswitching of the parent azobenzene at its typical wavelengths (**Fig 5d**: 20 to 400-fold slower green light photoswitching of **PST-30** at 520-540 nm, than switching of **MR69** at 540-560 nm), while the direct *E*→*Z* photoswitching is not substantially impaired. Assisted switching operates efficiently with RhB even at 600 nm, which has much better penetration into living tissue than wavelengths typically harnessed by azobenzenes.

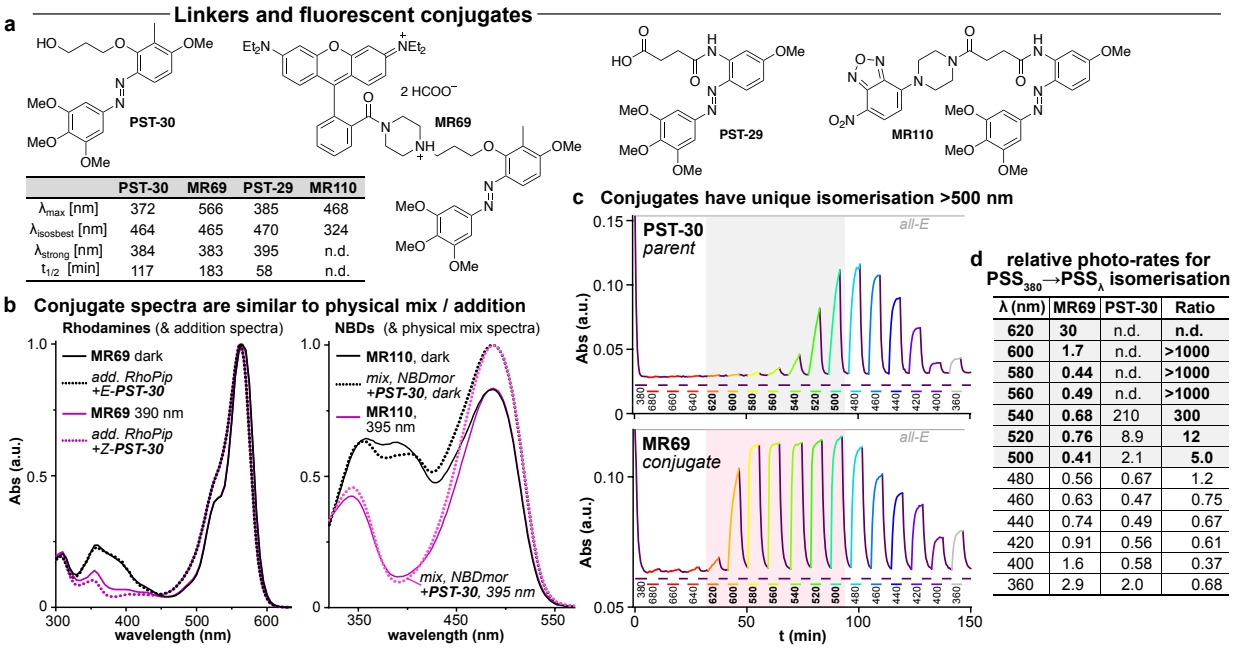

Figure 5. (a) Fluorophore conjugates **MR69** and **MR110** have **(b)** similar absorption features as the spectral sum of their components, but **(c,d)** undergo dramatically efficient and complete isomerisation when irradiated in the absorption region of their fluorophore motif. (n.d. indicates not measured; **c,d**: monochromator light source, 5 nm FWHM, see **Fig S4** for further details).

As the fluorophore motifs were capturing the energy used for this switching, we named this effect as *assisted* isomerisation. Excitingly, this can address general challenges that have troubled photopharmacology: e.g., how to achieve efficient isomerisation at long wavelengths, with a simple design for predictable photoresponse (here, at whatever wavelengths the fluorophore motif absorbs), *without* requiring drastic photoswitch redesign that blocks many substituent positions. For a brief discussion of the assisted switching design, rationale, and outcomes, see **Supporting Notes 2-5**; but since the mechanisms behind this effect turned out to be more complex than simple RET, we report their elucidation in two separate papers.[39,40] Because azobenzenes are popular quenchers for fluorescent probes, we think it likely that such assisted switching will have been *ongoing* before: but it seems that it was not necessarily measured and reported as such; and as far as we are aware, such conjugates have never before been trialled for photoswitching in biology under single photon excitation at wavelengths longer than those at which azobenzenes usually absorb. Thus, we briefly examined their biological performance.

As expected, installing linkers to give **PST-29/30** lowered potency (ether **PST-30** was still somewhat photoswitchably bioactive; **Fig 6a**). Unfortunately, the cellular localisation of conjugates **MR69** and **MR110** was dominated by their fluorophores' intrinsic distribution: delocalised lipophilic cation **MR69** to mitochondria (**Fig 6b**)[41], and hydrophobic NBD **MR110** in lipid vesicles (**Fig 6c**)[41]: thus, unsurprisingly, they did not stain MTs even after UV illumination. To test their target-binding, cell-free tubulin polymerisation assays were run at high[21] concentrations, but did not show inhibition (**Fig 6d,e**). We thus halted investigations, thinking that substantial fluorophore tuning would be needed for cellularly-useful assisted-switching tubulin photopharmaceuticals (discussion in **Conclusion** and **Supporting Note 4**).

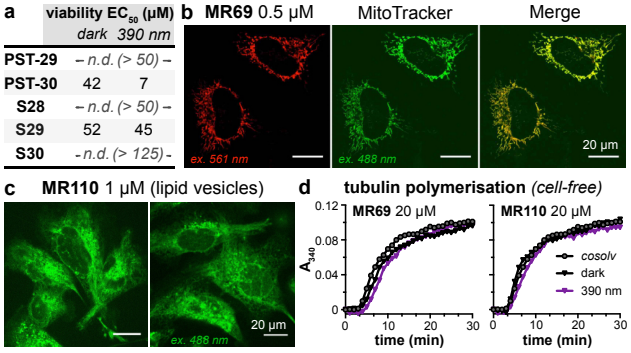

Figure 6. **(a)** Cytotoxicity of linker-**PSTs** (See **Supporting Note 1**). **(b,c)** In cells, **MR69** localises to mitochondria (c.f. MitoTracker Green), and **MR110** to lipid vesicles in the cytoplasm. (**a-c**: HeLa cells). **(d)** Neither **MR69** nor **MR110** inhibits tubulin polymerisation.

Conclusion

PSTs were previously used in photoswitching studies to disrupt MT polymerisation dynamics with spatiotemporal patterning, so applying spatiotemporally-defined gradients of antimitotic, anti-migratory, and cytotoxic effects in diverse cellular and *in vivo* models. To unlock higher performance photopharmacology, designs that have drastically improved photoswitching completeness and efficiency, are substantially more potent, and/or feature cargos allowing more elaborate chemical biology applications, are needed.

This photo-SAR study identified tolerances for modifications to the **PST** scaffold which can now be used

to adapt them for these needs: e.g., installing response to specific wavelengths, or avoiding it (wavelength orthogonality, e.g., blue-shifted **PST-27**); or tuning spontaneous relaxation speeds and polarity (**Fig 2**); which can be performed while keeping the *Z*-specific tubulin-binding cellular mechanism of action (**Figs 3-4**). This will support developing higher-performance **PST** reagents for microtubule studies; and we believe that even more blue-shifted (more GFP-orthogonal) reagents will prove to be the most valuable of those reagents.

We also found positions that may be suitable for attaching payloads, and used these to create fluorescent conjugates. We found these offered powerful solutions to the longstanding practical challenges of redshifting and high-completion isomerisation, which have hindered photopharmacology from *in vivo* application. The elucidation of the assisted switching mechanism is being reported elsewhere.[39,40] We think it likely that assisted switching will not actually prove impactful *within the **PST** series*: because **PSTs** are stoichiometric binders for a high-expression target (tubulin: ca. 10 μM in the cytosol[42]), so tubulin-inhibitory activity requires rather high concentrations of conjugates in the cytosol. Since most fluorophores are larger than the (moderate-potency) **PST** pharmacophore, we suspect that inevitable losses of potency upon payload attachment will be complicated by fluorophore biodistribution effects such that cellular applications as photoswitchably-binding *colchicinoids* are blocked (**Supporting Note 4**). However, we see strong scope for applications with (a) inherently high-potency scaffolds, since these may better tolerate fluorophore attachment; (b) reagents where incomplete *Z*→*E* switch-off has limited performance so far; (c) reagents being developed for use in deeper tissues, or in other optically dense or scattering systems including in materials, where long-wavelength response can be a great advantage.[39,40]

Supporting Information

*All methods, procedures, and **Supporting Notes** are given in the **Supporting Information**.*

Author Contributions

M.R., A.M.-D., K.K., A.R., and A.A. designed compounds, performed synthesis and analysis; M.G. performed and supervised cell-free and cellular assays; M.W. performed protein production, crystallization, compound soaking, X-ray data collection, processing, and structural refinement, as supervised by M.O.S.; L.O.R. and Y.K. performed cellular assays; K.S., A.J., and V.S. built the illuminating RFLM and performed online monitoring assays, as designed and supervised by P.P.; B.B. performed analysis; A.B. and T.S. performed synthesis; O.T.-S. designed the study and the targets, performed and supervised experiments, and wrote the manuscript with contributions from all authors.

Funding Statement

This project was supported by funds from the German Research Foundation (DFG: SFB 1032 *Nanoagents for Spatiotemporal Control* project B09 number 201269156; SFB TRR 152 project P24 number 239283807; SPP 1926 project XVIII number 426018126; and Emmy Noether grant TH2231/1-1 number 400324123; to O.T.-S.); the Munich Centre for NanoScience (CeNS: cooperation grant *PhotoWatcher* to P.P. and O.T.-S.); the Zentrales Innovationsprogramm Mittelstand (ZIM: Innovationsnetzwerke *Xellscreener* grant numbers 16KN092624 to P.P., 16KN092625 to A.J., 16KN092626 to O.T.-S.); the German Ministry of Economics and Industry (EXIST-Forschungstransfer project *CytoSwitch* number 03EFIBY145 to O.T.-S.); the Swiss National Science Foundation (31003A_166608 to M.O.S.).

Acknowledgements

MB acknowledges an LMUExcellent fellowship. We thank the LMU imaging platform CALM for microscopy access and Jörg Standfuss (PSI Villigen) for input and support for structural biology.

Conflicts of interest

K.S., A.J., and P.P. are employees of PHIO Scientific GmbH. All other authors declare no conflicts of interest.

Present Contact Addresses

M.G. (formerly LMU Munich) now at Ryvu Therapeutics, Leona Henryka Sternbacha 2, 30-394 Kraków, Poland. L.O.R. (formerly LMU Munich) now at Evotec GmbH, Neuried 82061, Germany.

References

(1) Dumontet, C.; Jordan, M. A. Microtubule-Binding Agents: A Dynamic Field of Cancer Therapeutics. *Nat Rev Drug Discov* **2010**, *9* (10), 790–803. https://doi.org/10.1038/nrd3253.

(2) Lian, Y.-L.; Lin, Y.-C. The Emerging Tools for Precisely Manipulating Microtubules. *Current Opinion in Cell Biology* **2024**, *88*, 102360. https://doi.org/10.1016/j.ceb.2024.102360.

(3) Wittmann, T.; Dema, A.; van Haren, J. Lights, Cytoskeleton, Action: Optogenetic Control of Cell Dynamics. *Current Opinion in Cell Biology* **2020**, *66*, 1–10. https://doi.org/10.1016/j.ceb.2020.03.003.

(4) Meiring, J. C. M.; Grigoriev, I.; Nijenhuis, W.; Kapitein, L. C.; Akhmanova, A. Opto-Katanin, an Optogenetic Tool for Localized, Microtubule Disassembly. *Current Biology* **2022**. https://doi.org/10.1016/j.cub.2022.09.010.

(5) Peterson, J. R.; Mitchison, T. J. Small Molecules, Big Impact: A History of Chemical Inhibitors and the Cytoskeleton. *Chemistry & Biology* **2002**, *9* (12), 1275–1285. https://doi.org/10.1016/S1074-5521(02)00284-3.

(6) Jordan, A.; Hadfield, J. A.; Lawrence, N. J.; McGown, A. T. Tubulin as a Target for Anticancer Drugs: Agents Which Interact with the Mitotic Spindle. *Medicinal Research Reviews* **1998**, *18* (4), 259–296. https://doi.org/10.1002/(SICI)1098-1128(199807)18:4<259::AID-MED3>3.0.CO;2-U.

(7) Mitchison, T. J. The Proliferation Rate Paradox in Antimitotic Chemotherapy. *MBoC* **2012**, *23* (1), 1–6. https://doi.org/10.1091/mbc.e10-04-0335.
(8) Pérez-Pérez, M.-J.; Priego, E.-M.; Bueno, O.; Martins, M. S.; Canela, M.-D.; Liekens, S. Blocking Blood Flow to Solid Tumors by Destabilizing Tubulin: An Approach to Targeting Tumor Growth. *J. Med. Chem.* **2016**, *59* (19), 8685–8711. https://doi.org/10.1021/acs.jmedchem.6b00463.
(9) Thorn-Seshold, O. Photoswitchable Cytotoxins. In *Molecular Photoswitches*; 2022; pp 873–919. https://doi.org/10.1002/9783527827626.ch36.
(10) Velema, W. A.; Szymanski, W.; Feringa, B. L. Photopharmacology: Beyond Proof of Principle. *J. Am. Chem. Soc.* **2014**, *136* (6), 2178–2191. https://doi.org/10.1021/ja413063e.
(11) Thorn-Seshold, O.; Meiring, J. C. M. Photocontrolling Microtubule Dynamics with Photoswitchable Chemical Reagents. In *Microtubules: Methods and Protocols*; Inaba, H., Ed.; Springer US: New York, NY, 2022; pp 403–430. https://doi.org/10.1007/978-1-0716-1983-4_26.
(12) Hamaguchi, M. S.; Hiramoto, Y. Analysis of the Role of Astral Rays in Pronuclear Migration in Sand Dollar Eggs by the Colcemid-UV Method. *Development, Growth & Differentiation* **1986**, *28* (2), 143–156. https://doi.org/10.1111/j.1440-169X.1986.00143.x.
(13) Wühr, M.; Tan, E. S.; Parker, S. K.; Detrich, H. W.; Mitchison, T. J. A Model for Cleavage Plane Determination in Early Amphibian and Fish Embryos. *Current Biology* **2010**, *20* (22), 2040–2045. https://doi.org/10.1016/j.cub.2010.10.024.
(14) Hadfield, J. A.; McGown, A. T.; Mayalarp, S. P.; Land, E. J.; Hamblett, I.; Gaukroger, K.; Lawrence, N. J.; Hepworth, L. A.; Butler, J. Substituted Stilbenes, Their Reactions and Anticancer Activity. WO2002050007A2, June 27, 2002.
(15) Bisby, R. H.; Botchway, S. W.; Hadfield, J. A.; McGown, A. T.; Scherer, K. M. Multi-Photon Isomerisation of Combretastatins and Their Use in Therapy. WO2013021208A2, February 14, 2013.
(16) Gao, L.; Meiring, J. C. M.; Kraus, Y.; Wranik, M.; Weinert, T.; Pritzl, S. D.; Bingham, R.; Ntouliou, E.; Jansen, K. I.; Olieric, N.; Standfuss, J.; Kapitein, L. C.; Lohmüller, T.; Ahlfeld, J.; Akhmanova, A.; Steinmetz, M. O.; Thorn-Seshold, O. A Robust, GFP-Orthogonal Photoswitchable Inhibitor Scaffold Extends Optical Control over the Microtubule Cytoskeleton. *Cell Chemical Biology* **2021**, *28* (2), 228-241.e6. https://doi.org/10.1016/j.chembiol.2020.11.007.
(17) Gao, L.; Meiring, J. C. M.; Varady, A.; Ruider, I. E.; Heise, C.; Wranik, M.; Velasco, C. D.; Taylor, J. A.; Terni, B.; Weinert, T.; Standfuss, J.; Cabernard, C. C.; Llobet, A.; Steinmetz, M. O.; Bausch, A. R.; Distel, M.; Thorn-Seshold, J.; Akhmanova, A.; Thorn-Seshold, O. In Vivo Photocontrol of Microtubule Dynamics and Integrity, Migration and Mitosis, by the Potent GFP-Imaging-Compatible Photoswitchable Reagents SBTubA4P and SBTub2M. *J. Am. Chem. Soc.* **2022**, *144* (12), 5614–5628. https://doi.org/10.1021/jacs.2c01020.
(18) Thorn-Seshold, O.; Borowiak, M.; Trauner, D.; Hasserodt, J. Azoaryls as Reversibly Modulatable Tubulin Inhibitors. WO2015166295A1, November 5, 2015.
(19) Seliwjorstow, A.; Takamiya, M.; Rastegar, S.; Pianowski, Z. Reversible Influence of Hemipiperazine Photochromism on the Early Development of Zebrafish Embryo. *ChemBioChem* **2024**, *n/a* (n/a), e202400143. https://doi.org/10.1002/cbic.202400143.
(20) Müller-Deku, A.; Meiring, J. C. M.; Loy, K.; Kraus, Y.; Heise, C.; Bingham, R.; Jansen, K. I.; Qu, X.; Bartolini, F.; Kapitein, L. C.; Akhmanova, A.; Ahlfeld, J.; Trauner, D.; Thorn-Seshold, O. Photoswitchable Paclitaxel-Based Microtubule Stabilisers Allow Optical Control over the Microtubule Cytoskeleton. *Nature Communications* **2020**, *11* (1), 4640. https://doi.org/10.1038/s41467-020-18389-6.
(21) Borowiak, M.; Nahaboo, W.; Reynders, M.; Nekolla, K.; Jalinot, P.; Hasserodt, J.; Rehberg, M.; Delattre, M.; Zahler, S.; Vollmar, A.; Trauner, D.; Thorn-Seshold, O. Photoswitchable Inhibitors of Microtubule Dynamics Optically Control Mitosis and Cell Death. *Cell* **2015**, *162* (2), 403–411. https://doi.org/10.1016/j.cell.2015.06.049.
(22) Singh, A.; Saha, T.; Begemann, I.; Ricker, A.; Nüsse, H.; Thorn-Seshold, O.; Klingauf, J.; Galic, M.; Matis, M. Polarized Microtubule Dynamics Directs Cell Mechanics and Coordinates Forces during Epithelial Morphogenesis. *Nat. Cell Biol.* **2018**, *20* (10), 1126–1133. https://doi.org/10.1038/s41556-018-0193-1.
(23) Engdahl, A. J.; Torres, E. A.; Lock, S. E.; Engdahl, T. B.; Mertz, P. S.; Streu, C. N. Synthesis, Characterization, and Bioactivity of the Photoisomerizable Tubulin Polymerization Inhibitor Azo-Combretastatin A4. *Org. Lett.* **2015**, *17* (18), 4546–4549. https://doi.org/10.1021/acs.orglett.5b02262.
(24) Sheldon, J. E.; Dcona, M. M.; Lyons, C. E.; Hackett, J. C.; Hartman, M. C. T. Photoswitchable Anticancer Activity via Trans–Cis Isomerization of a Combretastatin A-4 Analog. *Org. Biomol. Chem.* **2015**, *14* (1), 40–49. https://doi.org/10.1039/C5OB02005K.
(25) Rastogi, S. K.; Zhao, Z.; Barrett, S. L.; Shelton, S. D.; Zafferani, M.; Anderson, H. E.; Blumenthal, M. O.; Jones, L. R.; Wang, L.; Li, X.; Streu, C. N.; Du, L.; Brittain, W. J. Photoresponsive Azo-Combretastatin A-4 Analogues. *European Journal of Medicinal Chemistry* **2018**, *143*, 1–7. https://doi.org/10.1016/j.ejmech.2017.11.012.
(26) Eguchi, K.; Taoufiq, Z.; Thorn-Seshold, O.; Trauner, D.; Hasegawa, M.; Takahashi, T. Wild-Type Monomeric α-Synuclein Can Impair Vesicle Endocytosis and Synaptic Fidelity via Tubulin Polymerization at the Calyx of Held. *J. Neurosci.* **2017**, *37* (25), 6043–6052. https://doi.org/10.1523/JNEUROSCI.0179-17.2017.
(27) Kopf, A.; Renkawitz, J.; Hauschild, R.; Girkontaite, I.; Tedford, K.; Merrin, J.; Thorn-Seshold, O.; Trauner, D.; Häcker, H.; Fischer, K.-D.; Kiermaier, E.; Sixt, M. Microtubules Control Cellular Shape and Coherence in Amoeboid Migrating Cells. *Journal of Cell Biology* **2020**, *219* (6), e201907154. https://doi.org/10.1083/jcb.201907154.
(28) Zenker, J.; White, M. D.; Templin, R. M.; Parton, R. G.; Thorn-Seshold, O.; Bissiere, S.; Plachta, N. A Microtubule-Organizing Center Directing Intracellular Transport in the Early Mouse Embryo. *Science* **2017**, *357* (6354), 925–928. https://doi.org/10.1126/science.aam9335.
(29) Theisen, U.; Ernst, A. U.; Heyne, R. L. S.; Ring, T. P.; Thorn-Seshold, O.; Köster, R. W. Microtubules and Motor Proteins Support Zebrafish Neuronal Migration by Directing Cargo. *Journal of Cell Biology* **2020**, *219* (10), e201908040. https://doi.org/10.1083/jcb.201908040.
(30) Tron, G. C.; Pirali, T.; Sorba, G.; Pagliai, F.; Busacca, S.; Genazzani, A. A. Medicinal Chemistry of Combretastatin A4: Present and Future Directions. *J. Med. Chem.* **2006**, *49* (11), 3033–3044. https://doi.org/10.1021/jm0512903.
(31) Rempfler, M.; Stierle, V.; Ditzel, K.; Kumar, S.; Paulitschke, P.; Andres, B.; Menze, B. H. Tracing Cell Lineages in Videos of Lens-Free Microscopy. *Medical Image Analysis* **2018**, *48*, 147–161. https://doi.org/10.1016/j.media.2018.05.009.
(32) Gaspari, R.; Prota, A. E.; Bargsten, K.; Cavalli, A.; Steinmetz, M. O. Structural Basis of Cis- and Trans-Combretastatin Binding to Tubulin. *Chem* **2017**, *2* (1), 102–113. https://doi.org/10.1016/j.chempr.2016.12.005.

(33) Küllmer, F.; Gregor, L.; Arndt, H.-D. Systematic Modifications of Substitution Patterns for Property Tuning of Photoswitchable Asymmetric Azobenzenes. *Org. Biomol. Chem.* **2022**, *20* (20), 4204–4214. https://doi.org/10.1039/D2OB00214K.
(34) Medarde, M.; Maya, A. B. S.; Pérez-Melero, C. Review ArticleNaphthalene Combretastatin Analogues: Synthesis, Cytotoxicity and Antitubulin Activity. *Journal of Enzyme Inhibition and Medicinal Chemistry* **2004**, *19* (6), 521–540. https://doi.org/10.1080/14756360412331280473.
(35) Álvarez, C.; Álvarez, R.; Corchete, P.; Pérez-Melero, C.; Peláez, R.; Medarde, M. Exploring the Effect of 2,3,4-Trimethoxy-Phenyl Moiety as a Component of Indolephenstatins. *European Journal of Medicinal Chemistry* **2010**, *45* (2), 588–597. https://doi.org/10.1016/j.ejmech.2009.10.047.
(36) Jiang, S.; Crogan-Grundy, C.; Drewe, J.; Tseng, B.; Cai, S. X. Discovery of (Naphthalen-4-Yl)(Phenyl)Methanones and N-Methyl-N-Phenylnaphthalen-1-Amines as New Apoptosis Inducers Using a Cell- and Caspase-Based HTS Assay. *Bioorganic & Medicinal Chemistry Letters* **2008**, *18* (21), 5725–5728. https://doi.org/10.1016/j.bmcl.2008.09.088.
(37) Reddy, G. R.; Kuo, C.-C.; Tan, U.-K.; Coumar, M. S.; Chang, C.-Y.; Chiang, Y.-K.; Lai, M.-J.; Yeh, J.-Y.; Wu, S.-Y.; Chang, J.-Y.; Liou, J.-P.; Hsieh, H.-P. Synthesis and Structure−Activity Relationships of 2-Amino-1-Aroylnaphthalene and 2-Hydroxy-1-Aroylnaphthalenes as Potent Antitubulin Agents. *J. Med. Chem.* **2008**, *51* (24), 8163–8167. https://doi.org/10.1021/jm8008635.
(38) Wranik, M.; Weinert, T.; Slavov, C.; Masini, T.; Furrer, A.; Gaillard, N.; Gioia, D.; Ferrarotti, M.; James, D.; Glover, H.; Carrillo, M.; Kekilli, D.; Stipp, R.; Skopintsev, P.; Brünle, S.; Mühlethaler, T.; Beale, J.; Gashi, D.; Nass, K.; Ozerov, D.; Johnson, P. J. M.; Cirelli, C.; Bacellar, C.; Braun, M.; Wang, M.; Dworkowski, F.; Milne, C.; Cavalli, A.; Wachtveitl, J.; Steinmetz, M. O.; Standfuss, J. Watching the Release of a Photopharmacological Drug from Tubulin Using Time-Resolved Serial Crystallography. *Nature Communications* **2023**, *14* (1), 903. https://doi.org/10.1038/s41467-023-36481-5.
(39) Baumgartner, B.; Glembockyte, V.; Mayer, R.; Gonzalez-Hernandez, A.; Kindler, R.; Valavalkar, A.; Wiegand, A.; Müller-Deku, A.; Grubert, L.; Steiner, F.; Gross, C.; Reynders, M.; Grenier, V.; Broichhagen, J.; Hecht, S.; Tinnefeld, P.; Ofial, A.; Dietzek-Ivansic, B.; Levitz, J.; Thorn-Seshold, O. Azobenzenes Can Achieve Near-Infrared Photocontrol in Biological Systems, with Quantitative *Z→E* Photoisomerization, via Singlet Manifold Photoredox. *ChemRxiv* **2023**. https://doi.org/10.26434/chemrxiv-2023-37sv4.
(40) Baumgartner, B.; Glembockyte, V.; Gonzalez-Hernandez, A.; Valavalkar, A.; Mayer, R.; Fillbrook, L.; Müller-Deku, A.; Zhang, J.; Steiner, F.; Wiegand, A.; Gross, C.; Reynders, M.; Munguba, H.; Arefin, A.; Ofial, A.; Beves, J.; Lohmüller, T.; Dietzek-Ivansic, B.; Broichhagen, J.; Tinnefeld, P.; Levitz, J.; Thorn-Seshold, O. A General Method for Near-Infrared Photoswitching in Biology, Demonstrated by the >700 nm Photocontrol of GPCR Activity in Brain Slices. *ChemRxiv* **2024**. https://doi.org/10.26434/chemrxiv-2024-vm4n3.
(41) Reungpatthanaphong, P.; Dechsupa, S.; Meesungnoen, J.; Loetchutinat, C.; Mankhetkorn, S. Rhodamine B as a Mitochondrial Probe for Measurement and Monitoring of Mitochondrial Membrane Potential in Drug-Sensitive and -Resistant Cells. *Journal of Biochemical and Biophysical Methods* **2003**, *57* (1), 1–16. https://doi.org/10.1016/S0165-022X(03)00032-0.
(42) Jordan, M. A.; Thrower, D.; Wilson, L. Mechanism of Inhibition of Cell Proliferation by Vinca Alkaloids. *Cancer Res.* **1991**, *51* (8), 2212–2222.